Evaluation of history-matching methods for updating seismic derived models

Alexandre de Lima, Théophile Gentilhomme, David Riffault, Fabien Allo – CGG, Alessandra Anyzewski, Alexandre Emerick, Marcos Sebastião dos Santos – Petrobras

Abstract

This paper presents a comparison of two production history-matching methods using the UNISIM-I-H dataset. The objective is to evaluate the strengths and weaknesses of these methods when applied to seismic-derived models that already carry different sources of information. Both methods provide an estimation of the uncertainty by updating an ensemble of realizations. The quality of the data match, the preservation of the prior models and the ability of quantifying the uncertainties are used to compare the two methods. A first history matching is performed using the Ensemble Smoother with Multiple Data Assimilation (ES-MDA) method. A second history matching is performed using the Multi-Scale batch Levenberg-Marquardt ensemble Randomized Maximum Likelihood (MS-LM-enRML) method. While the ES-MDA perturbs the property fields grid-block by grid-block, the MS-LM-enRML uses wavelet re-parameterization in order to perturb those fields scale-by-scale and avoid unnecessary updates. Although a slightly better match is obtained with ES-MDA, MS-LM-enRML preserves better the prior models and the variability of the ensembles.

Introduction

The integration of different sources of information (well logs, geophysical and production data) helps reduce the uncertainty and improves the predictions of the reservoir models. However, when a sequential approach is followed, which is a common practice, it is important to preserve the information carried by the models when assimilating new data and keep a reasonably good estimation of the uncertainty. Production history matching is the last step of this workflow. Ensemble-based methods of optimization (Aanonsen et al., 2009) have gained popularity thanks to their flexibility, computational efficiency and ability to match dynamic data using a wide range of parameters. Ensemble-based methods also allow the estimation of posterior uncertainties using its ensemble of realizations. The ensemble is used to generate a linear regression model between the flow responses and the input parameters to update each individual ensemble member. However, this regression model is generally poorly constrained due to the limited size of the ensemble as a full fluid flow simulation needs to be run for each ensemble member. This can lead to a noisy update of the model parameters and an over-reduction of the ensemble variability due to the presence of spurious correlations in the regression model. As a consequence, geological or seismic-driven features can be damaged and the uncertainties provided by the ensemble are underestimated.

The objective of this paper is to evaluate the ability of two ensemble-based history-matching methods, the ES-MDA (Emerick and Reynolds, 2013) and MS-LM-enRML (Gentilhomme et al., 2015; Chen and Oliver, 2013), to preserve the prior information and quantify the uncertainty of the predictions while matching the historical production data. The UNISIM-I-H synthetic dataset (Avansi and Schiozer, 2015) used for this purpose spans over 10 years of production history. Porosity, net-to-gross and permeabilities are inverted along with initial fluid contact and relative permeabilities. The same ensemble of prior realizations and data error model are used with both methods and distance-based localizations, discussed in more detail in the following, are applied.

A short overview of the methods, focused on their differences, is provided in the following sections. Then the results of the different inversions are compared. Finally, the last section presents the conclusions of the paper.

Optimization methods

Both methods are derived from the enKF standard equation (Evensen, 2003), but instead of assimilating the time dependent data sequentially, the ES-MDA and MS-enRML uses all the data at one step, and the same data can be assimilated multiple times so that the update equation for each individual realization can be written as:

$$m_{j+1} = m_j + C_{MD}(C_D + C_{DD})^{-1}\left(d_{uc} - g(m_j)\right) \quad (1)$$
$$= m_j + K\left(d_{uc} - g(m_j)\right)$$

where C_{MD} is the $(n_p \times n_d)$ cross-covariance matrix (computed from the ensemble; Evensen, 2003; Aanonsen et al., 2009) between model parameters and the simulated responses, with n_p and n_d corresponding to the number of model parameters and data respectively; C_{DD} is the $(n_d \times n_d)$ auto-covariance matrix of the simulated responses; C_D is the $(n_d \times n_d)$ observed data error covariance matrix; d_{uc} is a $(n_d \times 1)$ vector of perturbed observation, i.e. $d_{uc} \sim N(d_{obs}, C_D)$ for MS-LM-enRML and $d_{uc} \sim N(d_{obs}, \alpha_j C_D)$ for ES-MDA, where N denotes a Gaussian distribution and d_{obs} is the $(n_d \times 1)$ observation vector; m_j and m_{j+1} represent $(n_p \times 1)$ vectors of parameters to be inverted (e.g. grid-block permeabilities, fluid contacts) for one given realization before and after assimilation of the data; $g(m_j)$ is the forward response

(e.g. simulated well production curves) with input parameters m_j and $K = C_{MD}(C_D + C_{DD})^{-1}$ is the Kalman gain.

Both ES-MDA and MS-enRML modify the inverse term of the Kalman gain at each iteration (i.e. at each assimilation of the data) in order to handle the non-linearity of the problem. The ES-MDA uses an inflation α_j coefficient so that:

$$K = C_{MD}(C_D + \alpha_j C_{DD})^{-1} \qquad (2)$$

whereas the MS-LM-enRML uses a Levenberg-Marquardt control parameter λ_j so that:

$$K = C_{MD}((\lambda_j + 1)C_D + C_{DD})^{-1} \qquad (3)$$

Although they are not modifying the Kalman gain the same way, the impact of α_j or λ_j is the same: they control the amplitude and orientation of the parameter updates in a trust-region (Byrd et al., 1987) way, i.e. by finding the best update in a limited region around the current state, which helps handle nonlinearity. Impact and control of these parameters are discussed in more details in (Emerick and Reynolds, 2013; Gentilhomme et al., 2015; Oliver et al., 2008). One difference, however, is that ES-MDA requires the sum of the inverse of α_j to be equals to one.

Parameterization and multi-scale approach

The main difference between ES-MDA and MS-LM-enRML comes from the parameterization of the spatial properties. ES-MDA works directly on the property values inside each grid-block the grid. All the parameters are perturbed for each assimilation step (equation 1).

With the MS-LM-enRML approach, the spatial properties are transformed in wavelet coefficients (Sweldens, 1998) The assimilation step (equation 1) is then performed on a subset of selected coefficients γ_{opt} of size $n_{opt} \leq n_p$, such that:

$$\begin{bmatrix} \gamma_{opt} \\ \gamma_{\overline{opt}} \end{bmatrix} = W.m \qquad (4)$$

where W, m, γ_{opt} and $\gamma_{\overline{opt}}$ correspond to the $(n_p \times n_p)$ wavelet transform matrix, the $(n_p \times 1)$ initial vector of grid-block values (e.g. porosity, permeability), the $(n_{opt} \times 1)$ vector of wavelet coefficients updated at the assimilation step and its complement vector respectively. For sake of simplicity, we assume here that m only contains spatial properties. Although we optimize only a subset of the coefficients, all coefficients are used to reconstruct the properties used by the flow simulator (Gentilhomme et al., 2015). Wavelet coefficients are both defined in space and frequency domains. Therefore, a scale-by-scale optimization process can be followed and a distance-based localization can be applied. This is discussed in more detail in the next section.

In the MS-LM-enRML method, a first set of large scale coefficients is initially selected and one (or several) assimilation step is performed by updating this subset. Then the parameterization is progressively refined, inserting finer scale coefficients in the optimization scheme until all the coefficients are included. The goal of this approach is to reduce the mismatch between the data and the simulated responses by only updating a very limited number of large coefficients in the first iteration, leaving the other scales unmodified. When the finer scale coefficients are finally included in the process, the amplitude of the perturbations are smaller as it is directly related to the amplitude of the mismatch (equation 1). More details about the MS-LM-enRML can be found in (Gentilomme et al., 2015).

Localization

Localization aims at regularizing the Kalman gain by removing the components affected by the spurious correlations inherent to the limited size of the ensemble used to construct it. Localization can be applied to the individual covariance matrices of the Kalman gain or directly to the Kalman gain itself (Chen and Oliver, 2010). The second approach (localization applied directly to Kalman gain itsel) is used in this work: a screen matrix A, containing elements in [0, 1], is applied to K such that:

$$\widetilde{K} = A \circ K \qquad (5)$$

Where $\widetilde{K}$ is the regularized Kalman gain and $\circ$ is the element wise Schur product. In distance-based localization, the elements of A are related to the separating distance of the data location (e.g. well locations) and spatial parameters (e.g. grid-blocks). Figure 2 shows an example of localization map. In this case, the elements of A smoothly decrease to zero with the separating distance. In other word, the impact of the data located in well PROD010 is greater close to the well than further away from it.

Standard distance-based localization method is applied in ES-MDA. A slightly different approach in followed in ML-LM-enRML. In this case, the localization functions are not fixed, but depend on the current scale being optimized (Figure 2). When only large scale coefficients are updated, the localization is less restrictive as the estimated correlations between the data and parameters are generally better (Chen and Oliver, 2012). However, the Kalman gain is more affected by spurious effects when all the coefficients are present. Accordingly, the localization becomes more restrictive. More information about multi-scale localization can be found in (Gentilhomme et al., 2015).

UNISIM-I-H example

UNISIM-I-H is a synthetic case based on Namorado's Field, located off-shore Brazil, in the Campos Basin. It is a sandstone reservoir (Figure 1) with ten years of production history, developed with 25 wells, 14 of which are producers and 11 of which are injectors. More details can be found in (Avansi and Schiozer, 2015).

Oil production rate, water-cut, bottom hole pressure and gas-oil ratio associated with measurement errors (Table

3) are used to constraint the inversion of the porosity, net-to-gross, horizontal permeability (PERMI) and vertical permeability (PERMK) fields (Table 1), along with flow parameters listed in the Table 2.
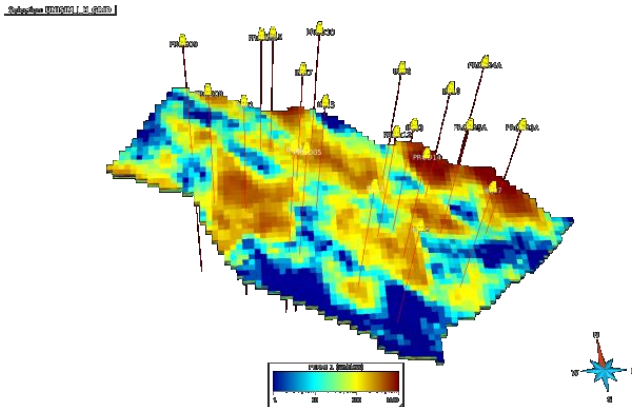

Figure 1 – UNISIM-I-H synthetic case.

An ensemble of 200 realizations has been generated by Sequential Gaussian Simulation using well logs hard data, whereas the prior values flow parameters are samples of truncated Gaussian distributions as described in Table 1 below.

Table 1 – Petrophysical parameters and its respective ranges.

Petrophysical Parameters		Log Transform	MIN	MAX
Porosity	[/]	No	0.01	0.35
Netgross	[/]	No	0	1
Horizontal Permeability (PERMI)	[mD]	Yes	0.1	3500
Vertical Permeability (PERMK)	[mD]	Yes	0.1	3500

Table 2 – Flow parameters and their respective distribution

Flow Parameters	Average Value	St. Dev	MIN	MAX
Water Oil Contact of Region 2	3174	50	3024	3324
Rock Compressibility (x E-5)	5.3	1.43	1	9.6
Vertical Permeability Multiplier	1.5	0.5	0	3
Relative Permeability – Corey Coefficients				
Critical Water Saturation (Swcr)	0.35	0.017	0.3	0.4
Max Water Relative Permeability (KRMAX)	0.35	0.067	0.15	0.55

Table 3 – List of observed data and their respective measurement errors

Observed Data	Error Type	ERROR	Minimum
Water Cut	Constant	0.05	-
Oil Production Rate (m3/day)	Fraction	5% of data	1
Bottom Hole Pressure (Kg/cm2)	Constant	10	
Gas Oil Ratio (sm3/sm3)	Fraction	20% of data	1

History-matching settings

As described before, the MS-LM-enRML iterates through different scales, starting with a reduced parameterization, whereas the ES-MDA directly starts with all the parameters. In both cases, a total number of 4 iterations are performed. The MS-LM-enRML iterates through 3

different scales. One iteration is performed at the two intermediate coarse scales and two iterations at the finest scale which includes the same number of parameters as ES-MDA.

Fixed distance-based localization is used in ES-MDA whereas scale-adaptive localization is used in MS-LM-enRML. Figure 2 shows an example of localization applied to the well PROD010 for all the different type of production data (Table 3Table 3 – List of observed data and their respective measurement errors).
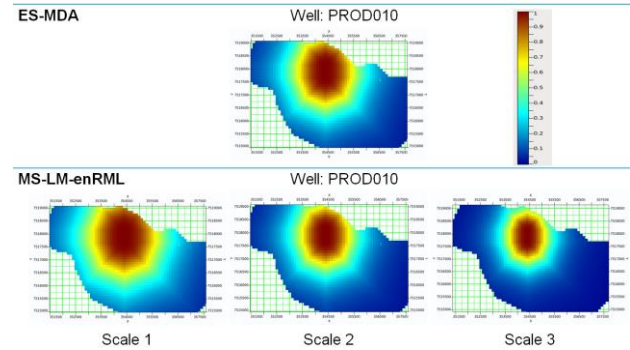

Figure 2 – Top: ES-MDA fixed localization for well PROD010. Bottom: scale-adaptive localization.

Comparative results

Histograms of objective function values for the different realizations of the ensemble are shown in Figure 3. ES-MDA achieves a slightly better match than MS-LN-enRML but both methods obtain satisfying misfits well within the data uncertainties (i.e. the objective function value is lower than 1). We can observe that most of the objective function values of ES-MDA are around 0.3, which reflect a homogenous match in the ensemble, whereas more variability is observed in MS-LM-enRML.
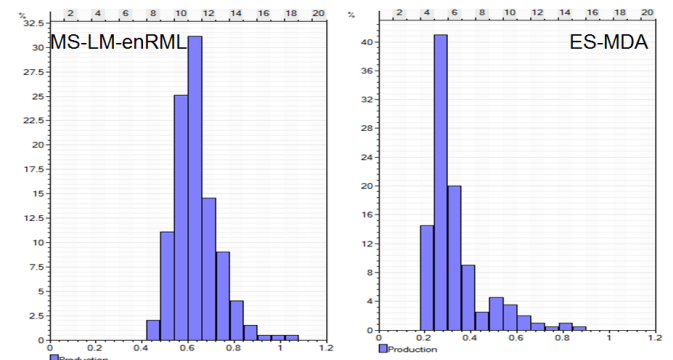

Figure 3 – Final objective function values.

Figure 4 shows the water cut final match and prediction for the well PROD005. ES-MDA, in agreement with the objective function values, reaches a better fit than MS-LM-enRML. However, more variability is observed with the MS-LM-enRML forecast compared to the ES-MDA, reflecting more variability in the ensemble.
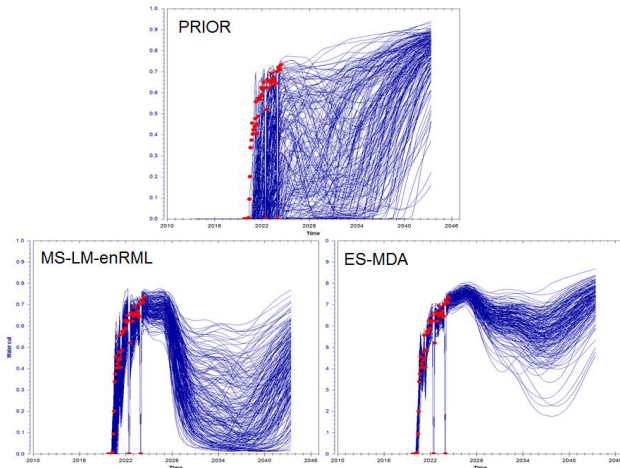
Figure 4 –Water cut curve of well PROD005.

Figure 5 shows the posterior distribution of the critical saturation and water-oil contact. Compared to the means and limits of the prior distributions given in Table 2, MS-LM-enRML seems to better preserve the distribution, whereas ES-MDA distributions hit the parameterization limits. Although the results obtained by MS-LM-enRML seem to act more reasonably, it is difficult to conclude on the quality of the results as the correct solution is unknown.
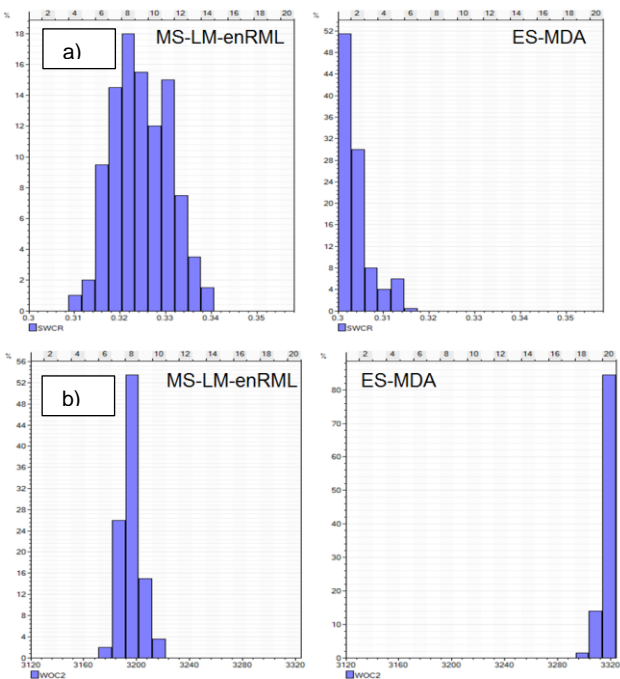

Figure 5 - a) Posterior distribution of the critical water saturation (SWCR) **b)** and initial Water-Oil contact (WOC).

The Figures 6 and 8 to 12 show the comparison between the prior and posterior (mean and standard deviation) for 200 realizations of each petrophysical properties.
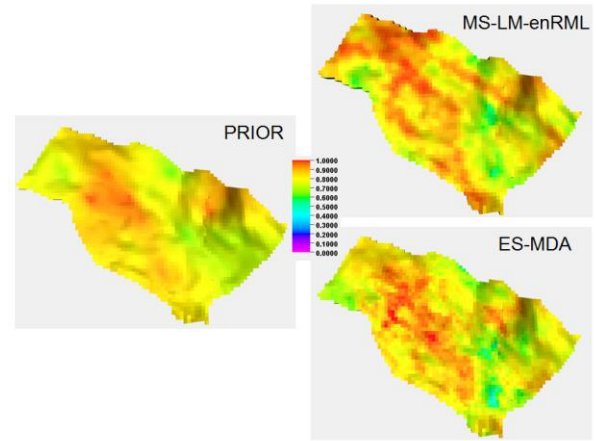

Figure 6 – Average maps of net-to-gross (Prior, MS-LM-enRML and ES-MDA).

Results are globally consistent between the two methods: similar features come out from the inversion in both cases (e.g. high porosity and permeability bodies south of the reservoir), although differences in the shape and amplitudes in values are visible. In both cases, the final values are reasonable, even though we can observe areas of large or low values. When looking at the average of the properties, the MS-LM-enRML better preserves the smoothness of the prior, whereas high frequencies are introduced in ES-MDA (Table 4). This can be quantified by using the ratio of energy r_e of the high-frequency coefficients (Gentilhomme et al., 2015) between the prior and final average properties:

$$r_e = \frac{e_x}{e_p}, \text{ with } e_x = \sum_{i \in \{HF\}} |\gamma_i| \qquad (6)$$

where e_x (e_p) is the final (initial) energy of the coefficients for the different properties and $\{HF\}$ represents a subset of high-frequency wavelet coefficients. An increase of the energy (i.e. ratio > 1) reflects addition of high-frequency content (i.e. noise) during the process.

Table 4 – Energy ratios of the properties

| Property name	Energy ratio r_e	
	MS-LM-enRML	ES-MDA
Porosity	1,43	2,76
Net-to-gross	2,63	5,96
Horizontal permeability	1,35	1,39

Presence of noisy high-frequencies in the average denotes the presence of spurious correlations which affect all the realizations in the same way. Although both methods show an increase of energy, this is less significant in the MS-LM-enRML case.

Finally, the standard deviations maps clearly show that the MS-LM-enRML better preserves the variability of the ensemble compared to ES-MDA. This may partially be explained by the fact ES-MDA obtains a slightly better match, but the authors believe that multi-scale approach helps minimizing the changes in the model parameters.

However, in term of preservation of the prior features, this example does not show major differences between the two methods. This can be explained by the fact that the prior realizations do not incorporate a large amount of data (no seismic data) and do not have features with sharp property contrast (e.g. channels).
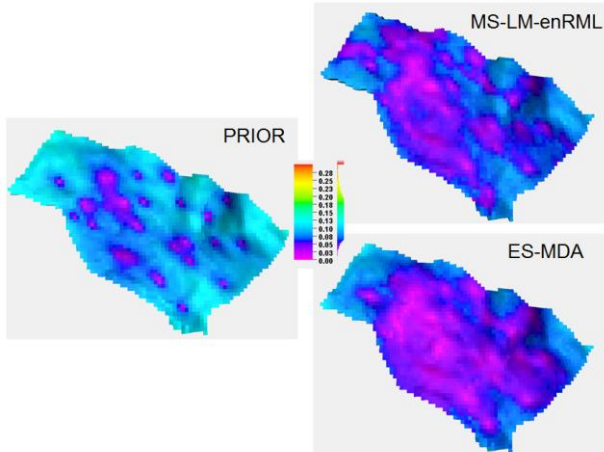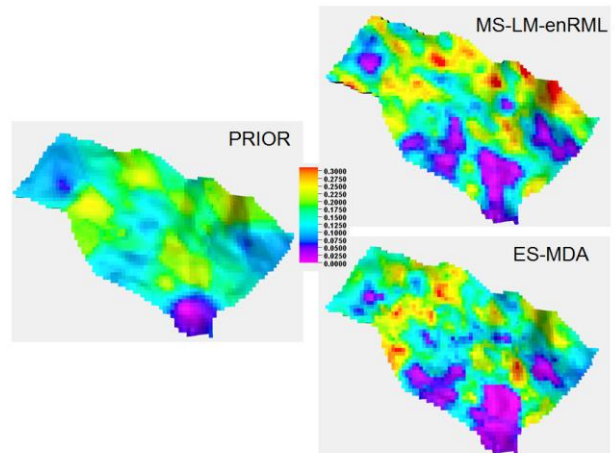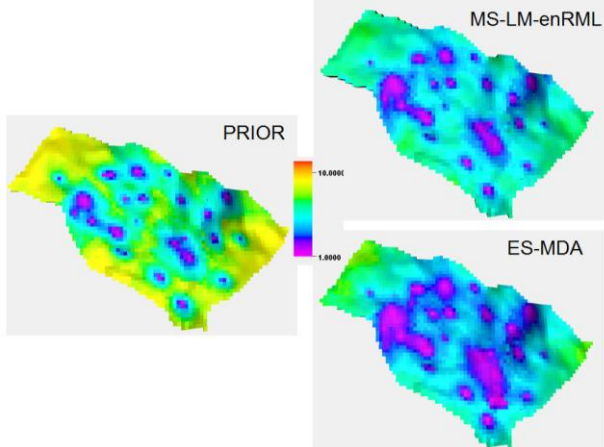

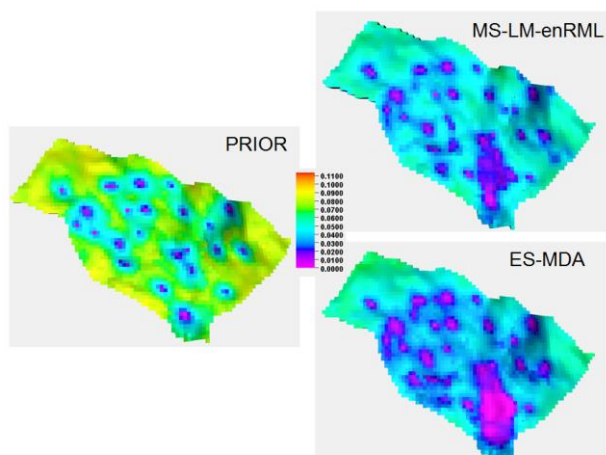**Figure 7 –** Standard deviation maps of net-to-gross (Prior, MS-LM-enRML and ES-MDA).
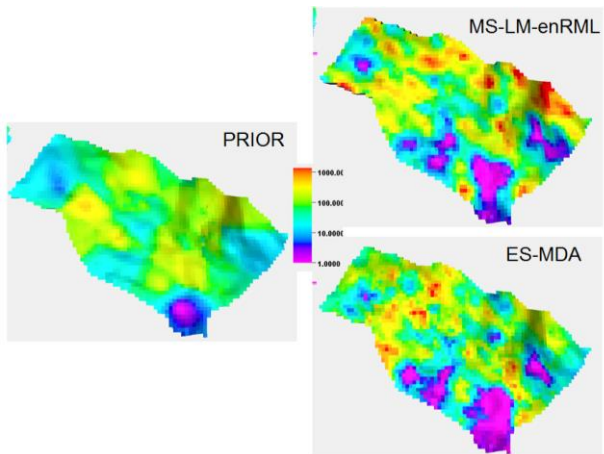
Figure 8 – Average (Top) and standard deviation maps (Bottom) of horizontal permeability (Prior, MS-LM-enRML and ES-MDA).
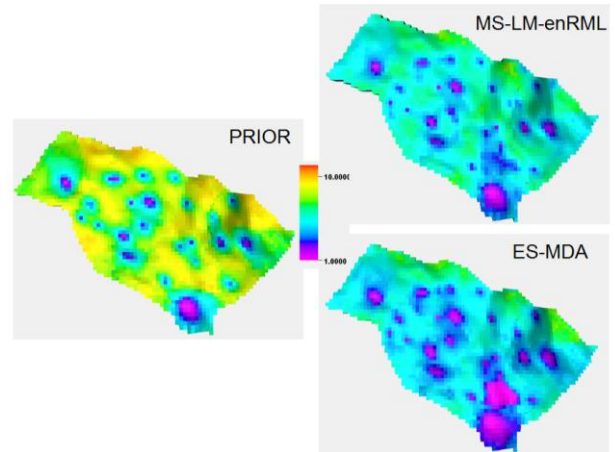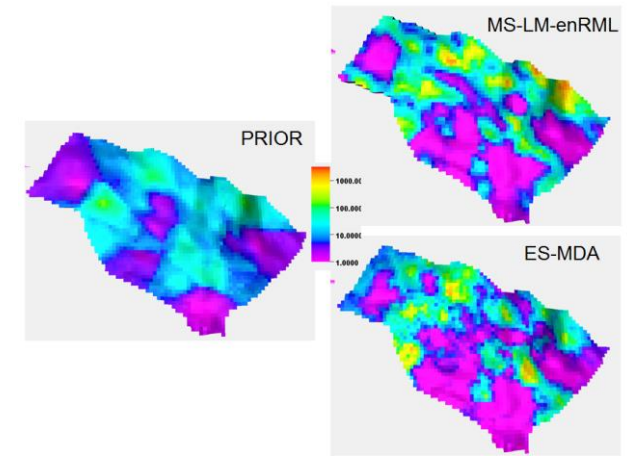
Figure 9 – Average (Top) and standard deviation maps (bottom) of vertical permeability (Prior, MS-LM-enRML and ES-MDA).


Figure 10 – Average maps of porosity (Prior, MS-LM-enRML and ES-MDA).

MS-LM-enRML

PRIOR

ES-MDA

Figure 11 – Standard deviation maps of porosity (Prior, MS-LM-enRML and ES-MDA).

Figure 13 illustrates one of the posterior realizations of net-to-gross after optimization by the two methods. MS-LM-enRML posterior realization preserves better the prior and is less noisy than ES-MDA.

MS-LM-enRML

PRIOR
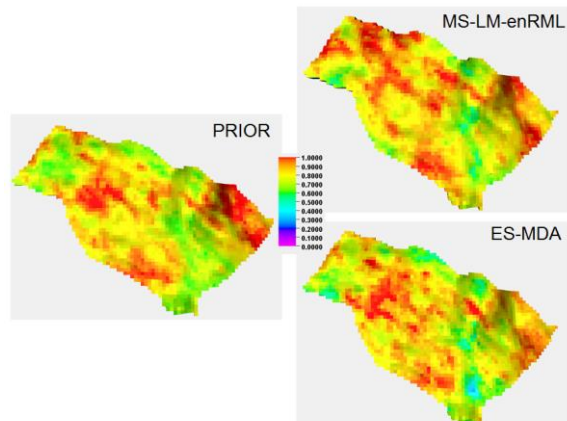
ES-MDA

Figure 12 – Posterior realization (n° 50) of net-to-gross.

Conclusions and discussions

Both ES-MDA and MS-LM-enRML provide a good match of the UNISIM-I-H data and return realistic output realizations while providing useful uncertainty in the prediction of the production. Although ES-MDA obtains a slightly better match after a fixed number of iterations, MS-LM-enRML better preserves the variability in the ensemble. It also limits the introduction of high-frequency noise in the realizations and obtains more variability in the production forecasts. Hence when dealing with seismic derived models, MS-LM-enRML might be more adapted as it tends to minimize the modifications of the model parameters and therefore helps preserve the prior information. However, when the prior ensemble is generated from stochastic process with little constraint, ES-MDA might be more appropriate as it obtains a better match with fewer iterations and the preservation of the models becomes less important.

When a large number of data is used to constrain the inversion, for example in 4D seismic history-matching,

one common issue with ensemble-based methods is the collapse of the ensemble (Emerick, 2013). Therefore MS-LM-enRML might be more appropriate in this situation as it better preserves the variability of the ensemble than ES-MDA.

Acknowledgments

References

Aanonsen, S. I.; Nævdal, G.; Oliver, D. S.; Reynolds, A. C. & Vallès, B., The Ensemble Kalman Filter in Reservoir Engineering---a Review, *SPE Journal,* **2009**, *14*, 393-412

Avansi, G. D., Schiozer, D. J., UNISIM-I: Synthetic Model for Reservoir Development and Management Applications, *International Journal of Modeling and Simulation for the Petroleum Industry*, **2015**, *9*, 21-30

Byrd, R. H.; Schnabel, R. B. & Shultz, G. A., A trust region algorithm for nonlinearly constrained optimization, *SIAM Journal on Numerical Analysis, SIAM,* **1987**, *24*, 1152-1170

Chen, Y. & Oliver, D. S., Cross-covariances and localization for EnKF in multiphase flow data assimilation, *Computational Geosciences, Springer Netherlands,* **2010***, 14*, 579-601

Chen, Y. & Oliver, D. S., Multiscale parameterization with adaptive regularization for improved assimilation of nonlocal observation, *Water resources research, Wiley Online Library,* **2012***, 48*

Chen, Y. & Oliver, D. S., Levenberg-Marquardt forms of the iterative ensemble smoother for efficient history matching and uncertainty quantification, *Computational Geosciences, Springer Netherlands,* **2013***, 17*, 689-703

Evensen, G., The Ensemble Kalman Filter: theoretical formulation and practical implementation, *Ocean Dynamics, Springer-Verlag,* **2003***, 53*, 343-367

Emerick, A. A. & Reynolds, A. C., History matching time-lapse seismic data using the ensemble Kalman filter with multiple data assimilations, *Computational Geosciences, Springer,* **2012***, 16*, 639-659

Emerick, A. A. & Reynolds, A. C., Ensemble smoother with multiple data assimilation, *Computers & Geosciences, Elsevier,* **2013***, 55*, 3-15

Emerick, A. A., Analysis of the Performance of Ensemble-based Assimilation of Production and Seismic Data, *Journal of Petroleum Science and Engineering, Elsevier,* **2013***, 139*, 219-239

Gentilhomme, T.; Oliver, D. S.; Mannseth, T.; Caumon, G.; Moyen, R. & Doyen, P., Ensemble-based multi-scale history-matching using second-generation wavelet transform, *Computational Geosciences,* **2015***, 19*, 999-1025

Oliver, D. S.; Reynolds, A. C. & Liu, N., Inverse theory for petroleum reservoir characterization and history matching *Cambridge University Press,* **2008**

Sweldens, W., The lifting scheme: A construction of second generation wavelets, *SIAM Journal on Mathematical Analysis, [Philadelphia] Society for Industrial and Applied Mathematics.,* **1998***, 29*, 511-546